JOURNAL OF THERMOPHYSICS AND HEAT TRANSFER
Vol. 8, No. 2, April–June 1994

Rocket Plume Base Heating Methodology

John E. Reardon*
REMTECH, Inc., Huntsville, Alabama 35805
and
H. F. Nelson†
University of Missouri—Rolla, Rolla, Missouri 65401

A review of radiative transport calculation methods for base heating is presented followed by a description of the current methodology for the Space Shuttle plume radiation predictions and improvements for the advanced solid rocket booster (ASRB). The calculation methods include empirical methods, the standardized infrared radiation model code, and the forward and reverse Monte Carlo methods. Current plume radiation methods include those used for the Space Shuttle main engines and the solid rocket booster (SRB). Methods being developed for the ASRB include changes in plume property prediction methodology and application of the reverse Monte Carlo method in predicting plume radiation models. Results of the prediction methods are compared with experimental measurements on the current SRB and on $\frac{1}{6}$-scale motors using both SRB and ASRB propellants. Examples are also presented demonstrating the statistical results available with the reverse Monte Carlo method.

Introduction

THIS article presents a review of the current methods used to predict base heating of rockets caused by exhaust plume radiation. Plume radiation prediction is also of interest in defining signatures for target detection and tracking, but the signature prediction is more restricted both spatially and spectrally. The plume signature typically is detected at distances of the order of kilometers, and special features of the spectra are important. The lines of sight between the detector and the plume are essentially parallel and of the same length. In contrast, the base of the rocket views the plume from close-in, so lines of sight between the detector and the plume have large ranges in angle and length. The near plume, just downstream of the exhaust nozzle exit, is most important in the heating problem, while the far plume is of secondary importance.

Prediction of radiative base heating for the Space Shuttle is currently of great interest because advanced solid rocket motor (ASRM) boosters have a new propellant that has a greatly increased radiation potential. The aluminum mass fraction is being increased from 16% for the redesigned solid rocket motors (RSRM) currently used on the Space Shuttle to 19% for the ASRM. This increase, combined with a smaller binder fraction, increases both the Al_2O_3 concentration and the plume temperature. The combined effects increase the plume radiation base heating of the ASRM approximately 30% relative to the RSRM.

Gaseous combustion products in solid propellant plumes radiate weakly compared to the plume particles, so the radiation is strongly dependent upon the properties of the particles. Calculation of the radiation emitted by the plume requires an accurate model of the plume flowfield, including the flowfield physics, the radiation properties of the plume gases, and the optical properties of the plume particulates. Currently, the Joint Army-Navy-NASA-Air Force (JANNAF) standard plume flowfield (SPF-II) code is the most up-to-date plume flowfield prediction code available.[1]

Engineering Methods

Radiative base heating of a rocket by its exhaust plume has been actively investigated for several years. Reviews of the state-of-the-art of the base heating problem prior to 1966 were published by Rochelle[2] and Carlson.[3] Engineering models for practical calculations of plume radiation have been developed by Fontenot,[4] Morizumi and Carpenter,[5] Bartkey and Bauer,[6] and Bobco and Edwards.[7] The current baseline method for base heating predictions[8,9] of the Shuttle solid propellant motor plume radiation is based on work by Bobco,[10,11] Edwards,[12] and Edwards and Bobco.[13] It models plume emission as being from effectively opaque conical surfaces. The radiation is described in terms of radiosity, which varies axially along the plume.

Edwards et al.[14] formulated an improved engineering model to predict the radiosity of conical-shaped plumes. The local incident radiant flux is the effective plume radiance scaled by the geometric view-factor from an opaque surface approximating the plume shape. Two free parameters in the model are evaluated by matching data from space firings of solid rocket motors. This approach is currently used with the effective plume radiance determined from flight measurements. However, this is not a predictive methodology because no a priori estimates can be given for the plume radiance. Rather, it is a means of interpolating or extrapolating the measurement at one base location to others, accounting for geometric effects.

Standard Infrared Radiation Model

The standardized infrared radiation model (SIRRM) was developed by JANNAF to provide a state-of-the-art computer code to calculate the infrared radiation signature of tactical and strategic rocket plume flowfields. The plume flowfield serves as input to SIRRM. The accuracy of the SIRRM calculations depends entirely on the accuracy of the plume flowfield. SIRRM accounts for anisotropic scattering, coupled emission, absorption and scattering by an inhomogeneous mixture, and contains a very large particle and gas data base. Some assumptions in SIRRM make it inappropriate for base heating calculations. A few of these assumptions are 1) radiation calculations are along parallel lines-of-sight, 2) plume

Received June 3, 1993; presented as Paper 93-2823 at the AIAA 28th Thermophysics Conference, Orlando, FL, July 6–9, 1993; revision received Aug. 16, 1993; accepted for publication Aug. 25, 1993.

*Senior Program Manager.
†Professor of Aerospace Engineering, Thermal Radiative Transfer Group, Department of Mechanical and Aerospace Engineering and Engineering Mechanics. Associate Fellow AIAA.

axial property variations are only partially accounted for, and 3) radiation emitted at forward aspect angles (between 0–30 deg) is weighted trigonometrically. Even so, SIRRM has been used to predict base heating, with some success.[15]

SIRRM includes both gas-band modeling and particulate emission and scattering. This was done in a fairly rigorous manner for the simplified case of "two-flux" scattering (scattering in the forward and rear hemispheres). An extension of this development was made to include the "six-flux" scattering (scattering in the six orthogonal directions surrounding the particle: forward, backward, and four side directions). The six-flux model accounts for situations in which the spectral radiance along a line-of-sight is affected by the properties of the entire volume, not just the properties along the line-of-sight.

Pearce et al.[15] made predictions and measurements of radiative base heating from a solid propellant rocket motor plume. The predictions were based on the SPF-II and SIRRM-II codes. Experimental measurements of spectrally resolved radiation were obtained using a subscale test motor and they showed that most of the radiative base heating was due to the Al_2O_3 condensed phase particles in the 1–2-μm spectral range. The SIRRM-II predictions were least accurate in this range and underpredicted the plume radiance by about a factor of 2, but better agreement might be expected with more recent optical properties.

Radiation Transport Calculation Methods

Monte Carlo

Monte Carlo analysis of plume radiative heating consists of following photons, or bundles of energy, from their point of emission in the plume until they leave the plume and hit or miss the surface area where the heat transfer is being calculated. The place of birth of the photon and the outcome of each event along its trajectory is determined using an appropriate probability distribution function. When the photon leaves the plume, it is traveling in a specific direction and it either hits or misses the base area of interest. This process is repeated a large number of times until statistically relevant data are obtained. Monte Carlo simulation will provide solutions to any radiative transfer problem if given enough computer time. However, the accuracy is dependent upon the accuracy of the flowfield property predictions and the optical properties of the particles.

Stockham and Love[16] used a Monte Carlo method to determine the radiation heat transfer to the exterior base region of a finite cylindrical volume of absorbing, emitting, and anisotropically scattering particles. They showed that the difference between anisotropic and isotropic scattering was important for cylinder optical diameters (optical thickness based on cylinder diameter) less than about 2. They also showed that searchlight effects can play an important role in radiative base heating.

Watson and Lee[17] used a Monte Carlo method to model the thermal radiation field for solid rocket plumes. The model accounted for axial and radial property variations of both the particles and the gases in the plume. The scattering was allowed to be either isotropic or anisotropic.

Reverse Monte Carlo

Nelson[18,19] used a reverse Monte Carlo method to predict the radiation from conical-shaped emitting, scattering media. This method 1) is more computationally efficient than forward Monte Carlo because all the rays are counted, 2) is easily applied to rocket plume base heating, and 3) readily accounts for searchlight radiative heating.

The reverse Monte Carlo method is used to predict radiation to a specific point. In reverse Monte Carlo, rays initially travel in a direction opposite to the direction in which they physically propagate. Mathematically, a ray is originated from a point on the receiver in the opposite direction from which the radiation emitted from the plume travels. The ray is followed through the plume, from event to event as it interacts with the gases and particles. Eventually, it is either absorbed in the plume, or escapes through the plume boundary. Rays that escape are assumed to be lost, unless they escape into the rocket exhaust nozzle, consequently contributing to searchlight emission. Rays that are absorbed in the plume are assumed to represent emission at the point, x, where they are absorbed. The radiance of the ray is equal to $I_{b\lambda}[T(x)]$, where $I_{b\lambda}$ is the Planck function, $T(x)$ is the temperature of the absorber at point x, and λ is the wavelength. The emitted energy then retraces its incident path forward in time until it emerges from the plume at the point where it was originally incident on the plume, but in the opposite direction. This method considers only rays that are incident on the point at which the radiation heat transfer is being calculated; consequently, it is more computationally efficient than direct Monte Carlo.

Wang[20] and Everson and Nelson[21] used reverse Monte Carlo to predict rocket plume base heating. Both papers show good agreement with experimental measurements. The largest source of error in the method is due to uncertainties in flowfield predictions and particle optical properties.

Reed and Calia[22,23] reviewed rocket particle properties with an aim toward prediction of visible, ultraviolet, and infrared radiation from aluminized solid propellant rocket plumes. Their work provides a summary of the research previously performed and an extensive set of references on the thermophysical properties of Al_2O_3.

Current Predictions

Reardon et al.[24] recently reviewed the status of base heating predictions for the Space Shuttle. They also discussed expected changes for the ASRM in heating magnitudes and calculation models. Table 1 presents general parameters for several current rocket motors. Particle radiation is very important for ASRM; however, it is difficult to calculate because of scattering. Monte Carlo methods are advantageous for radiation calculations involving scattering, because they easily model radiation scattering and allow insight into the sensitivity of the radiation to parameters in the calculations.

Base thermal environments are critical for the Space Shuttle because of the large surface area to be protected. Design specifications currently being prepared require radiation predictions at approximately 1700 locations. Additional predictions at many of these locations will also be required for two Space Shuttle main engine (SSME) failure conditions. The

Table 1 Motor/propellant comparison

	Nozzle				Propellant fractions		
			Radius, cm				
Motor	Type	Area ratio	Throat	Exit	Al	Ammonium perchlorate	Binder
ORSRM	Contour	7.16	69.1	184.9	0.16	0.70	0.14 PBAN
SRM/RSRM	Contour	7.73	68.3	190.0	0.16	0.70	0.14 PBAN
ASRM	Contour	7.73	68.3	190.0	0.19	0.69	0.12 HTPB
MNASA 2 and 4/RSRM	Conical	5.85	12.6	30.6	0.16	0.70	0.14 PBAN
MNASA 3 and 6/ASRM	Contour	7.59	12.6	34.8	0.19	0.69	0.12 HTPB

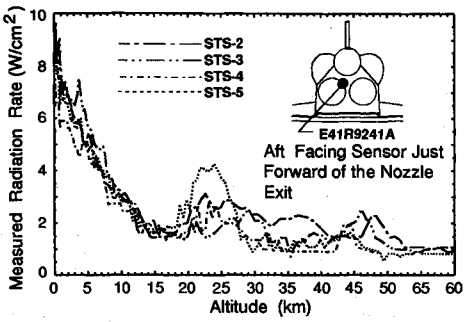

Fig. 1 SSME plume radiation heating rate characteristics.

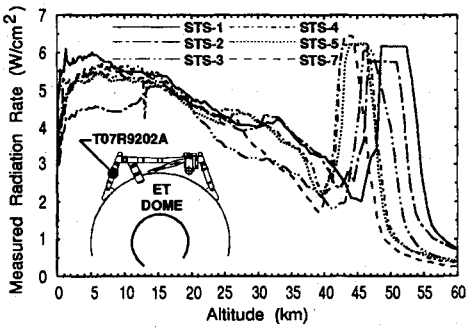

Fig. 2 OSRB plume radiation heating rate characteristics.

base thermal environments must also include factors representing the sensitivity of predicted nominal heating rate to nozzle gimbal angle for six control patterns (plus and minus pitch, yaw and roll) using the design envelope of gimbal angles.

Radiation from the SSME is from the H_2O bands. It is significant at sea level because of the very hot compression region behind the Mach disks and afterburning at the plume boundaries. The radiation heating rates diminish rapidly with altitude and are generally low above 15 km. Typical flight measurements for a radiometer attached to an SSME nozzle are illustrated in Fig. 1. SSME plume radiation is predicted using gas band-model methods with axisymmetric plume models at 0-, 6.1-, 12.2-, and 48.8-km altitudes. These predictions are used to define a sea-level heating rate and to select 1 of 10 adjustment functions to predict the radiative heating for the 0–12.2-km range. Between 12.2–48.8 km the radiation heating rate is assumed to vary linearly with altitude. The radiative heating rate at 48.8 km is predicted using a three-dimensional plume model and this rate remains valid above 48.8 km because the base pressure remains nearly constant.

The SRM plume radiation heating rate is very high at sea level and increases up to 30% for the 3–9-km altitude range. From 9 to 25 km, the radiation heating rate decreases with altitude, but between 25–35 km, flow separation and flow reversal bring plume boundary gases into the base region which increases the heating rate. Above 35 km the SRM radiation heating rate decreases until SRM shutdown, where a significant spike in radiation heating rate occurs. This behavior is shown in Fig. 2 for an instrument on the external tank (ET)/orbiter attachment structure. The variation with altitude is due to flow phenomena which are not currently modeled by theoretical methods. Consequently, adjustment functions for the altitude based on flight experience are used. These adjustments are a function of flight trajectory parameters, and they are applied to the radiation rates derived from a sea-level plume radiation model. The existing Space Shuttle solid rocket motor (SRM) methodology uses a single, conservative, sea-level plume radiation model and two adjustment functions: one based on altitude and one based on time to separation (for the shutdown spike). The sea-level plume radiation model is a 15-deg cone consisting of 10 axial nodes. Each node is approximately one nozzle-exit-radius in length, and its emissive power is determined by a combination of measurements and Monte Carlo predictions to give an axial distribution for emissive powers which varies from 79 to 24 W/cm^2. The emissive powers of nodes near the nozzle are adjusted to agree with ground-test measurements of radiance normal to the plume which are blended with predictions made with a Monte Carlo code[17,25,26] for downstream nodes.

Advanced Solid Rocket Motor Radiant Heating Methodology

The current radiative heating methodology follows the development of the advanced solid rocket booster (ASRB) plume radiation models from the cycle 1 model in 1990–91 (for selected critical heating points), to the cycle 1.5 model in 1991–92 (for the ET), to the cycle 2 model (for the ASRM, orbiter, and SSME nozzles) just being completed. For each cycle, the goal is to produce a plume property model which can be used with Monte Carlo predictions to certify that the predictions match ground tests and flight results at sea level. These methods are then used to predict a view-factor model for the original Space Shuttle solid rocket motor/booster (OSRB), and the results are compared with flight measurements to define factors to compensate for surface reflections and functions to adjust for altitude effects. The same methodology is then used to derive a similar ASRB radiation model which is used with the adjustments derived for the OSRB to predict the base heating environments.

In this process, the reverse Monte Carlo code is normally used with the "rocket" particle index of refraction data base from SIRRM. Most of the spectra from 400 to 10,000 cm^{-1} are integrated using 400-cm^{-1} intervals. However, some regions with strongly varying absorption, such as the CO_2-CO band near 4800 cm^{-1}, use a 200-cm^{-1} interval. In the range from 10,000 to 17,000 cm^{-1}, where there is no significant gas radiation, two intervals of 2000 and one of 3000 cm^{-1} are used.

During cycle 1, plume models did not match the radiation heating levels of available OSRB ground and flight test data, so the ratio of ASRB-to-OSRB predictions was used to adjust the OSRB plume model heating rates to those appropriate for the ASRB plume.[27] Also, the current altitude function was modified slightly to reflect the changes in trajectory.

Modified Plume Models

In the period between cycle 1 and cycle 1.5, several radiation measurements were made in the solid propellant test article (SPTA) (same as MNASA) test series at NASA Marshall Space Flight Center (MSFC) and on two test and evaluation motor (TEM) firings. (TEM firings use SRMs equivalent to the current RSRM, but without the latest case design.) Evaluation of the test results and prediction methods indicated that the gas-particle heat transfer coefficient and the particle size had a large effect on the predictions and a large uncertainty in the parameters being used, and prudent adjustments in these parameters produced good agreement with the measurement results. The cycle 1.5 plume model used a heat-transfer coefficient of one-half the normal value, and the mean particle size was adjusted to 1.5 times the Hermsen correlation value.[24] Five particle-size bins were used in the plume. An average particle density of 3.5 g/cm^3 was used because the codes did not consider particle size changes with density as the particles solidify. Comparisons of ground tests and predictions using these changes will be described later.

Cycle 1.5 Predictions

The 15-deg cone model was retained for the cycle 1.5 sea-level radiation model to facilitate predictions. Emissive powers at the nodes were predicted using the modified plume models and a Monte Carlo prediction at the center of each node. In performing the integration at the center of each node, a hemisphere was placed on the interior of the cone at

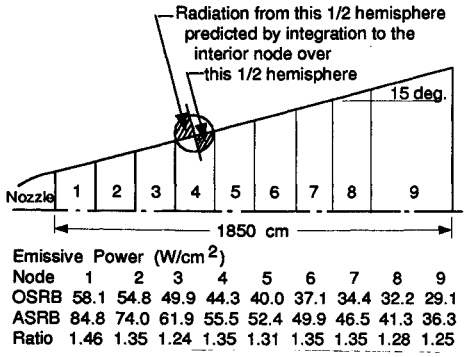

Emissive Power (W/cm^2)

Node	1	2	3	4	5	6	7	8	9
OSRB	58.1	54.8	49.9	44.3	40.0	37.1	34.4	32.2	29.1
ASRB	84.8	74.0	61.9	55.5	52.4	49.9	46.5	41.3	36.3
Ratio	1.46	1.35	1.24	1.35	1.31	1.35	1.35	1.28	1.25

Fig. 3 Sea-level plume model for cycle 1.5 and the node emissive power.

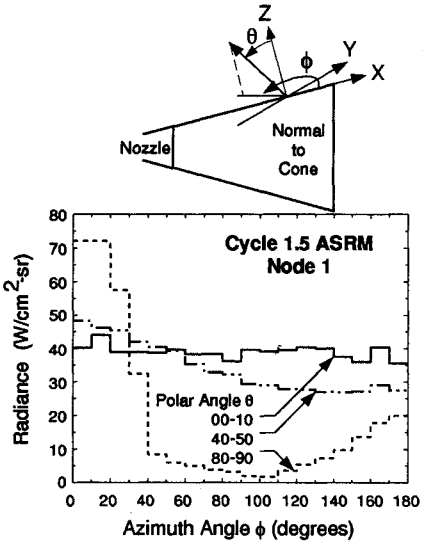

Fig. 4 Typical angular variations of radiance for the first node of the cycle 1.5 ASRM (Fig. 3). The angle ϕ is in the *XY* plane.

the center of the node, and the angular limits on the integration were set to include only the downstream half of the hemisphere on the interior as illustrated in Fig. 3. This was considered to be the best estimate of the average emissive power of the cone exterior as seen from the ET base region. The radiative heating rate predicted for the OSRB agreed with sea-level flight data for three sensors on the aft portion of the ET base. However, predictions for sensors at more forward locations on the ET base were too low. An estimate of reflections from the SRB and Orbiter body flap surfaces indicated that they produce radiative heating increases which were consistent with the relative magnitude of the differences between the predictions and flight results. As a result, the ET base region was divided into zones, each represented by a sensor. A "ratio" was assigned to each zone to adjust the heating prediction for reflections.[28] These ratios were then used to adjust similar predictions for the ET surfaces using the ASRB plume model. Altitude and shutdown spike functions were fitted to the flight data in each zone using functions of chamber-to-altitude pressure ratio, chamber pressure, and time to separation.[29] Gimbal adjustments were made on the normal (nonfailure) predictions, and the final results were published by Reardon[30] and Bender et al.[31]

Cycle 2 Prediction

As this article is being prepared, plume radiative heating models have not been finalized for cycle 2 predictions, but the modeling procedure has been selected. The plume models will use an improved gas-particle heat transfer correlation[32] which produces the same trends as the cycle 1.5 assumption of one-half the normal correlation. The mean particle size is uncertain at this time, but the particle distribution function will be modified to match the distribution function measured in the downstream portions of plumes during the MNASA test series at MSFC.[33] The sea-level radiation model will be based on Monte Carlo predictions of radiance at each plume node as a function of elevation and azimuth angle supplied as tables in 10-deg increments in each angle. Figure 4 illustrates typical variations using the cycle 1.5 plume mode, and the variation at $\theta = 0$–10 is primarily an indication of statistical errors in the Monte Carlo results for the number of rays used. The refinement from integrated radiance to an angle function was made to produce the increased precision needed to predict both forward aspects toward the base region and near-normal aspects toward the adjacent ASRB. It is anticipated that reflection factors will continue to be required to match the sea-level predictions with flight results for some regions of the base region.

Comparisons with Experiments

In order to certify the cycle 1.5 prediction methodology, comparisons were made with a large number of measurements on the MNASA 2–6 and TEM motor firings. The geometry used to describe the measurement is illustrated in Fig. 5. An instrument position is specified by the aspect angle and the aim point.

The MNASA motors are fired vertically, so instruments with an unrestricted view (wide angle) were used to evaluate the overall prediction, while measurements were made with a narrow-view instrument to aid in diagnostics. The TEM motors are fired horizontally, and the resulting disturbance of the plume and radiation reflections off of the ground make interpretation of wide-angle measurements difficult. As a result, TEM tests include off-axis, narrow-view measurements to evaluate plume boundary predictions. However, gimballing of the nozzle during the tests and difficulty in aiming these instruments increase the uncertainty in evaluating the test results.

Comparisons of the MNASA and TEM measurements with cycle 1.5 predictions are shown in Figs. 6 and 7. The on-axis, narrow-view measurements and predictions for both the MNASA and TEM motors compare well, except for the measurements aimed into the nozzle at the 120-deg aspect. However, the wide-angle comparisons for the MNASA motors and the off-axis comparisons for the TEM motors are marginal. These results indicate a possible problem in flowfield or radiation predictions near the plume boundary. A lack of absorption in the boundary is consistent with inadequate predicted attenuation of the radiation from the nozzle at the 120-deg aspect.

Plume models have been improved in preparation for cycle 2 predictions, but the apparent inadequate emission/absorption problem in the plume boundary remains. Analytical efforts to remedy this problem are directed at evaluating the methods used by the SPF-II code to treat particles near the boundary. Experimental efforts are directed at evaluating effects of gas species on the optical properties of the particles which might indicate a change in optical properties depending upon composition variations in the plume. Some recent comparisons of spectral results from MNASA tests indicate good agreement with the cycle 2 methodology, but comparisons between sea-level predictions and flight measurements are currently uncertain because of effects of radiometer window

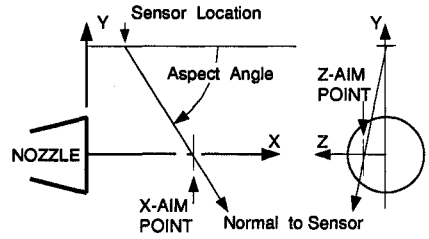

Fig. 5 Sensor geometry parameters.

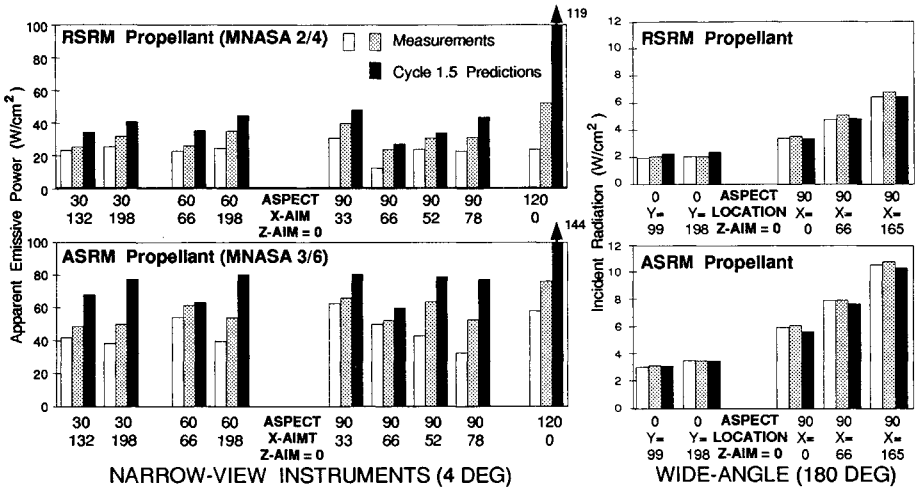

Fig. 6 Comparison of measurements and predictions for MNASA 2/4 (RSRM) and 3/6 (ASRM). Note the 120-deg aspect predictions extend to 119 and 144 W/cm². Aim points are in cm.

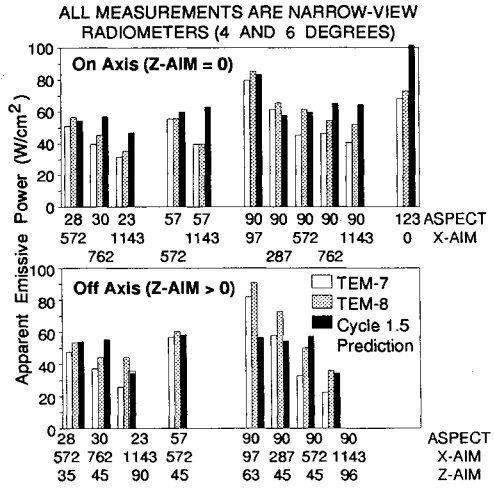

Fig. 7 Comparison of measurements and predictions for TEM 7 and 8. Aim points are in cm.

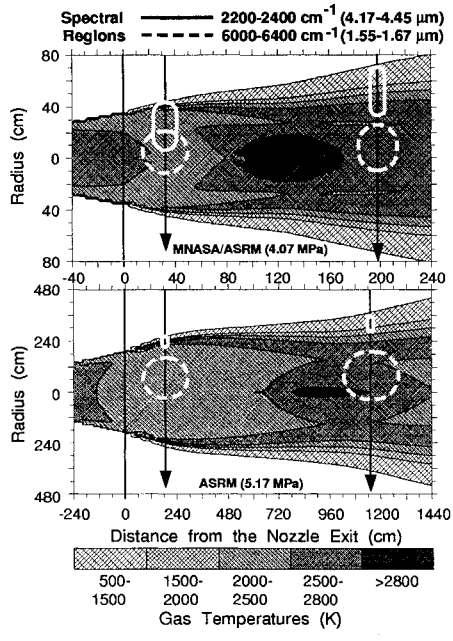

Fig. 8 Examples of Monte Carlo statistical results on regions of importance for CO_2 and particulate emission bands for two different sized motors.

on the calibration results and the methods used for flight data reduction. It appears that the cycle 1.5 predictions might overpredict flight results that are correctly interpreted for spectral effects of the radiometer window, while cycle 2 predictions, which are slightly lower, are more realistic.

Monte Carlo Statistical Data

The reverse Monte Carlo method provides statistical information on the source and location of emission for each ray and these data have been used to improve understanding of the plume structure and the sources of radiation from the plume. Some examples, which have been shown previously,[21] include the regions of significant particle and gas radiation in plumes of various scale and the source of spectral radiation—gas, particle, or nozzle wall.

An example showing regions of relative importance for the MNASA and full-scale ASRM plumes is illustrated in Fig. 8. The data are from predictions for narrow-view (4–6 deg) radiometers viewing normal to the plume across its diameter at similar locations. The centers of the regions represent the average distance from the sensor to the emission location. The length of each region represents the standard deviation of the distance to the emission location, while the width represents the average radius of the emission location from the center of the conical view into the plume. The illustration indicates that the emission for the strong CO-CO_2 band (4.17–4.45 μm) occurs primarily in the plume boundary, and the relative size of the region is much smaller on the larger plume. In contrast, emission in the 1.56–1.67-μm region, where particle emission is most significant, occurs near the center of the plume. In this spectral band, in the reverse Monte Carlo sense, many of the rays entering the small plume scatter back out without being absorbed, while in the larger plume a smaller fraction of the rays escapes. The result is a much larger region for emission for the full-scale motor, even though it appears to be about the same size on a relative scale. In the forward Monte Carlo sense, these regions represent the location of the radiation sources which are the primary contributors to the radiation as seen from locations outside the plume. These regions for particle radiation tend to be near the plume center where the temperatures and densities are the highest.

The example of spectral contributions in Fig. 9 is for the narrow-view (4-deg) radiometer location nearest to the MNASA/ASRM nozzle exit shown in Fig. 8. The total radiation predicted to the sensor was 0.1075 W/cm², neglecting window absorption. Here, particles are the primary radiators except in the stronger gas bands, and the importance of the nozzle wall is relatively small. The overall searchlight radiation for the case illustrated in Fig. 9 is shown in Fig. 10. The searchlight radiation consists of contributions from both the

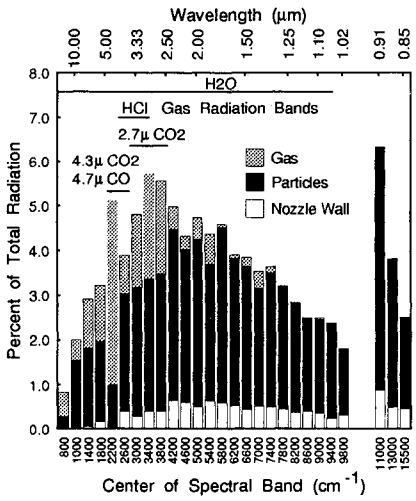

Fig. 9 Gas, particle, and nozzle-wall contributions to total radiation predicted for the MNASA/ASRM plume at a 90-deg aspect, 1-nozzle exit radius downstream of the nozzle. The integrated radiance from the plume is 28.1 W/cm².

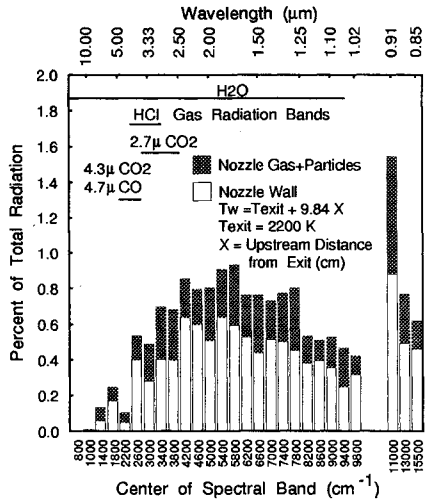

Fig. 10 Predicted SRM searchlight spectra and emission sources for the same condition as Fig. 9. Searchlight is 16.3% of the total radiation.

nozzle wall and the gas and particles in the nozzle. (Note that the wider bands, above 10,000 cm^{-1}, appear to be relatively strong because the results are in percent of total radiation rather than spectral radiance.)

Future Goals

Current project-oriented funding is not sufficient for full development of the new numerical and theoretical concepts needed for future radiative base heating applications. Plans should be pursued to integrate the current improvements into future thermal models of vehicle structure which will be feasible as computer power increases. CFD improvements will allow calculation of three-dimensional flowfield models with both gaseous and two-phase plumes. These flowfield models would be used as input to a reverse Monte Carlo code to predict angular distribution of radiation for a convenient network of nodes surrounding the plumes. Ray-traced three-dimensional displays could give thermal designers a visual picture of the radiation field which could help them to take advantage of surface coatings and structural shading in optimizing the thermal protection system. Realization of these improvements will require a coordinated program to define and develop the component analytical tools. Experiments are also necessary to continue to improve the understanding of particle properties, turbulence, and particle-gas heat transfer processes in plumes.

Acknowledgments

The work reported here on the ASRB environment predictions has been supported by the NASA Marshall Space Flight Center, Huntsville, Alabama, under Contracts NAS8-37891 and NAS8-39235, monitored by Peter Sulyma. The methods developed have been a cooperative effort of many persons in the plume technology community. Persons especially helpful have included Lee Foster and Peter Sulyma of the MSFC Thermal Environment Branch, who have promoted the development of the new methods in the face of pressures to continue the use of existing methods based on purely empirical methods and/or SIRRM technology; Bob Reed, who suggested the reverse Monte Carlo approach; John Everson, who developed our current code; Fred Nelson, who served as consultant for development of the current methods; and Sheldon Smith and Bruce Moylan, who have ably managed the plume property predictions.

References

[1]Dash, S. M., Pergament, H. S., Wolf, D. E., Sinha, N., Taylor, M. W., and Vaughn, M. E., "The JANNAF Standardized Plume Flowfield Code, Version II," Vols. I and II, U.S. Army Missile Command, Redstone Arsenal, AL, July 1990.

[2]Rochelle, W. C., "Review of Thermal Radiation from Liquid and Solid Propellant Rocket Exhausts," NASA Rept., TMX 53579, Feb. 1967.

[3]Carlson, D. J., "Radiation from Rocket Exhaust Plumes, Part II: Metalized Solid Propellant Exhaust Plumes," AIAA Paper 66-652, June 1966.

[4]Fontenot, J. E., Jr., "Thermal Radiation from Solid Rocket Plumes at High Altitude," *AIAA Journal*, Vol. 3, No. 5, 1965, pp. 970–972.

[5]Morizumi, S. J., and Carpenter, H. J., "Thermal Radiation from the Exhaust Plume of an Aluminized Composite Propellant Rocket," *Journal of Spacecraft and Rockets*, Vol. 1, No. 5, 1964, pp. 501–507.

[6]Bartky, C. D., and Bauer, E., "Predicting the Emittance of a Homogeneous Plume Containing Alumina Particles," *Journal of Spacecraft and Rockets*, Vol. 3, No. 10, 1966, pp. 1523–1527.

[7]Bobco, R. P., and Edwards, D. K., "Radiation from an Absorbing Scattering Conical Dispersion with Non-Uniform Density," Aerospace Technology Research Rept., SSD 60571R, Hughes Aircraft Co., Los Angeles, CA, 1966.

[8]Greenwood, T. F., Lee, Y. C., Bender, R. L., and Carter, R. E., "Development of Space Shuttle Base Heating Methodology and Comparison with Flight Data," *Proceedings of the JANNAF 13th Plume Technology Meeting*, Chemical Propulsion Information Agency, CPIA Publication 357, Vol. I, Houston, TX, April 1982, pp. 67–81.

[9]Greenwood, T. F., Lee, Y. C., Bender, R. L., and Carter, R. E., "Space Shuttle Base Heating," *Journal of Spacecraft and Rockets*, Vol. 21, No. 4, 1984, pp. 339–345.

[10]Bobco, R. P., "Radiation from Conical Surfaces with Nonuniform Radiosity," *AIAA Journal*, Vol. 4, No. 3, 1966, pp. 544–546.

[11]Bobco, R. P., "Reply by Author to D. K. Edwards on Radiation from Conical Surfaces with Nonuniform Radiosity," *AIAA Journal*, Vol. 7, No. 8, 1969, p. 1659.

[12]Edwards, D. K., "Comment on Radiation from Conical Surfaces with Nonuniform Radiosity," *AIAA Journal*, Vol. 7, No. 8, 1969, pp. 1656–1659.

[13]Edwards, D. K., and Bobco, R. P., "Effect of Particle Size Distribution on the Radiosity of Solid Propellant Rocket Plumes," *Spacecraft Radiative Transfer and Temperature Control*, edited by T. E. Horton, Vol. 83, Progress in Astronautics and Aeronautics, AIAA, New York, 1982, pp. 169–188.

[14]Edwards, D. K., Sakurai, Y., and Babikan, D. S., "A Two-Particle Model for Rocket Plume Radiation," *Journal of Thermophysics and Heat Transfer*, Vol. 1, No. 1, 1987, pp. 13–20.

[15]Pearce, B. E., Wurster, W. H., Flanigan, M. C., Smolarek, K. K., and Huang, R., "Predictions and Measurements of Radiation Base Heating from a Solid Propellant Rocket Motor Plume," AIAA Paper 91-1431, June 1991.

[16]Stockham, L. W., and Love, T. J., "Radiative Heat Transfer from a Cylindrical Cloud of Particles," *AIAA Journal*, Vol. 6, No. 10, 1968, pp. 1935–1940.

[17]Watson, G. H., and Lee, A. L., "Thermal Radiation Model for Solid Rocket Plume Radiation," *Journal of Spacecraft and Rockets*, Vol. 14, No. 11, 1977, pp. 641–647.

[18]Nelson, H. F., "Backward Monte Carlo Modeling for Rocket

Plume Base Heating," JANNAF Exhaust Plume Technology Meeting, Redstone Arsenal, AL, May 1991.

[19]Nelson, H. F., "Backward Monte Carlo Modeling for Rocket Plume Base Heating," *Journal of Thermophysics and Heat Transfer*, Vol. 6, No. 3, 1992, pp. 556–558.

[20]Wang, K. C., "Prediction of Rocket Plume Radiative Heating Using Backward Monte Carlo Method," AIAA Paper 93-0137, Jan. 1993.

[21]Everson, J., and Nelson, H. F., "Development and Application of a Reverse Monte Carlo Radiative Transfer Code for Rocket Plume Base Heating," AIAA Paper 93-0138, Jan. 1993.

[22]Reed, R. A., and Calia, V. S., "Review of Rocket Particle Properties Research," Arnold Engineering Development Center Rept., AEDC-TR-89-11, Nov. 1989.

[23]Reed, R. A., and Calia, V. S., "Review of Aluminum Oxide Rocket Particles," AIAA Paper 93-2419, July 1993.

[24]Reardon, J. E., Everson, J., Smith, S. D., and Sulyma, P. R., "ASRM Radiation and Flowfield Prediction Status," JANNAF Exhaust Plume Technology Meeting, Redstone Arsenal, AL, May 1991.

[25]Carter, R. C., "Space Shuttle Solid Rocket Booster Thermal Radiation Model," Lockheed LMSC-HREC TR D568530, Dec. 1978.

[26]Greenwood, T. F., "Improved SRM Plume Radiation Design Heating," Marshall Space Flight Center, ED33-80-45 (LMSC-HREC TR D698084), Nov. 1980.

[27]Reardon, J. E., and Everson, J., "ASRM Cycle 1 Plume Radiation Methodology," REMTECH, Inc., RTN 213-09, Huntsville, AL, Feb. 1991.

[28]Reardon, J. E., Everson, J., and Fulton, M. S., "Cycle 1.5 ASRB Sea-Level Plume Radiation Model Description," REMTECH, Inc., RTN 250-1-05, Huntsville, AL, March 1992.

[29]Reardon, J. E., and Fulton, M. S., "Development of Cycle 1.5 ASRB Plume Radiation Altitude and Shutdown-Spike Adjustment Functions," REMTECH, Inc., RTN 250-1-06, Huntsville, AL, March 1992.

[30]Reardon, J. E., and Fulton, M. S., "Cycle 1.5 ASRB Plume Radiation Reference Sea-Level Environments," REMTECH, Inc., RTN 250-1-07, Huntsville, AL, March 1991.

[31]Bender, R. L., Brown, J. R., Fulton, M. S., and Reardon, J. E., "Cycle 1.5 ASRB Ascent Base Heating Environments for the External Tank," REMTECH, Inc., RTN 250-2-01, Huntsville, AL, Feb. 1992.

[32]Moylan, B. E., and Sulyma, P., "Nusselt Number Correlations for Solid Rocket Motors," 20th Plume Technology Subcommittee Meeting, Chemical Propulsion Information Agency, CPIA Publication 595, Vol. 1, Feb. 1993, pp. 59–70.

[33]Sambamurthi, J., "Plume Particle Collection and Sizing from MNASA Motor Tests in Support of Thermal Radiation Analysis," NASA ED33-100-92, Aug. 1992.